

ENABLING QUANTUM CYBERSECURITY ANALYTICS IN BOTNET DETECTION: STABLE ARCHITECTURE AND SPEED-UP THROUGH TREE ALGORITHMS

 Madjid Tehrani,
  Eldar Sultanow,
  William J Buchanan,
  Malik Amir,
  Anja Jeschke,
  Raymond Chow, and
  Mouad Lemoudden

ABSTRACT. For the first time, we enable the execution of hybrid machine learning methods on real quantum computers with 100 data samples and real-device-based simulations with 5,000 data samples, thereby outperforming the current state of research of Suryotrisongko and Musashi from 2022 who were dealing with 1,000 data samples and quantum simulators (pure software-based emulators) only. Additionally, we beat their reported accuracy of 76.8% by an average accuracy of 91.2%, all within a total execution time of 1,687 seconds. We achieve this significant progress through two-step strategy: Firstly, we establish a stable quantum architecture that enables us to execute HQML algorithms on real quantum devices. Secondly, we introduce new hybrid quantum binary classification algorithms based on Hoeffding decision tree algorithms. These algorithms speed up the process via batch-wise execution, reducing the number of shots required on real quantum devices compared to conventional loop-based optimizers. Their incremental nature serves the purpose of online large-scale data streaming for DGA botnet detection, and allows us to apply hybrid quantum machine learning to the field of cybersecurity analytics. We conduct our experiments using the Qiskit library with the Aer quantum simulator, and on three different real quantum devices from Azure Quantum: IonQ, Rigetti, and Quantinuum. This is the first time these tools are combined in this manner.

CONTENTS

1. Introduction	2
2. Background	4
2.1. DGA Botnets	4
2.2. Machine Learning	5
2.3. Hybrid Quantum Machine Learning	5
2.4. Quantum Machine Learning	6
3. Methodology	7

Key words and phrases. Quantum, Cybersecurity Analytics, Machine Learning, Botnet, Hoeffding Tree.

3.1. Selected Platforms	7
3.2. Description of the Dataset	7
4. Stable Architecture for Long-running Experiments	9
4.1. Reasons for Instability	9
4.2. Stabilized Architecture	10
4.3. Quantum-enhanced Hoeffding Tree Classifier (QHTC)	12
5. Experimental Results	15
5.1. Execution Time and Accuracy	15
5.2. Performance Metrics of QHTC	16
6. Conclusion and Future Work	18
Appendix A. Pseudo-code Algorithms	21
Appendix B. Glossary	25
References	27
List of Figures	30
List of Tables	31
List of Referenced Lists	32

1. INTRODUCTION

In the rapidly evolving digital landscape where cyber threats are growing both in sophistication and pervasiveness, maintaining robust cybersecurity measures has taken center stage. While traditional cybersecurity approaches remain effective to a degree, they often struggle to keep up with the constant flood of cyber-attacks [1]. In recent years, machine learning has proven to be valuable in various cybersecurity applications. It's been effective in tasks such as intrusion detection, malware classification, and anomaly detection by harnessing automated data analysis and pattern recognition capabilities [2]. Now, the rise of quantum computing is paving the way for even further improvements in cybersecurity analytics.

Quantum computing, renowned for its ability to perform intricate computations at a speed exponentially faster than traditional computers [3], shows promising potential to revolutionize cybersecurity. Quantum machine learning, which has emerged as the intersection of quantum computing and machine learning, leverages the distinctive properties of quantum systems to devise innovative algorithms with the potential to outperform their classical counterparts [4]. In this paper, we explore the domain of quantum-enhanced cybersecurity analytics, with a special focus on employing quantum machine learning algorithms for botnet detection - a pressing cybersecurity issue with significant implications for network security [5]. By utilizing the power of quantum

computing, we aim to establish a stable architecture and capitalize on the prospective speed enhancement offered by tree algorithms, thereby strengthening the effectiveness and efficiency of botnet detection methods.

The term *Cybersecurity Analytics* [6, 7] refers to the application of data analysis techniques to cybersecurity. Much of the literature on this subject takes a practical approach, offering tangible examples and implementable code for cybersecurity solutions [8, 9, 10]. However, a term that encapsulates cybersecurity analytics within the context of a quantum system, such as *Quantum Cybersecurity Analytics*, is yet to be fully coined. This is a goal of our present work. In this paper, we introduce *Quantum Cybersecurity Analytics*, or QCA, as a field that employs quantum technology, particularly quantum machine learning, to devise cybersecurity solutions.

We address the challenges and computational demands inherent to quantum machine learning algorithms through the creation of a stable architecture and the adaptation of the Hoeffding tree algorithm for incremental learning [11]. The current state of the art defined in [12] shows the classification with a hybrid approach of 1000 data samples on a quantum simulator from a botnet dataset with an accuracy of 76.8%, whereas the total execution time is not reported. In their study, no signs of any real-device-based simulations or even computations on real quantum devices is shown. We outperform these achievements in the following ways:

- (1) We have extended the maximum sample size from 1,000 to 5,000 data samples in a quantum machine learning method, using real-device-based simulation through the Quantum Hoeffding Tree Classifier (QHTC) algorithm. Our method achieves an average accuracy of 91.2% and a final-round accuracy of 100%, all within a total computation time of 1,687 seconds, which is on par with the total execution time observed in locally deployed quantum simulations.
- (2) Furthermore, and for the first time, we implemented various Hybrid Quantum Binary Classification (HQBC) algorithms on actual quantum devices. We managed to process a maximum of 100 randomly fixed data samples, achieving a top accuracy of 59.0%.

In addition, our work makes the following additional contributions:

- (1) We overcome the pitfalls due to the instabilities of long-running code on three different Azure Quantum Providers by code hardening.
- (2) We apply the batch-wise Hoeffding Tree algorithm instead of the usual loop-wise algorithms relying on gradient descent.
- (3) We compare a diverse set of binary classifiers on real devices, on real-device-based simulations as well as quantum simulators. All experiments are conducted consistently using the IEEE Botnet DGA dataset.
- (4) Quantum Cybersecurity Analytics is made possible.

The source code implementation is publicly available at [13]. The subsequent sections of this paper are organized as follows: Section 2 delves into the background of DGA botnets and machine learning for cybersecurity. The details of our methodology are described in Section 3. In Section 4, the requirements for a stable architecture to run QML algorithms are identified and the quantum-enhanced Hoeffding tree classifier is introduced. In Section 5, the experimental results are presented. Finally, Section 6 serves as the conclusion of this paper.

2. BACKGROUND

In this section, we present an overview of the following subjects and delve into the difficulties and possibilities linked to each one: domain generation algorithms (DGAs) botnets, the utilization of machine learning, hybrid quantum machine learning, and quantum machine learning for the detection of botnets through network traffic data.

2.1. DGA Botnets. A botnet refers to a network of computers infected and controlled by a single attacker, known as the botmaster [14, 15]. Consequently, combatting and addressing botnets has become an important issue, as they have become a prevalent method for launching various internet-based attacks, such as spam, phishing, click fraud, key logging and cracking, copyright infringements, and Denial of Service (DoS) [16]. The communication topologies that pose the greatest threat to Command-and-Control (C&C) servers are Domain Generation Algorithm (DGA), peer-to-peer (P2P), and hybrid structures. Our primary focus lies in examining the communication patterns and protocols employed by DGA botnets. Extensive research on these communication patterns has been conducted by the authors of [17]. To detect malicious domains, we adopt domain name detection techniques. The literature offers a comprehensive study of DGA botnets, which serves as a baseline use case for exploring quantum machine learning, given the well-understood patterns of malicious activities in DGA botnets.

A DGA-based botnet is an advanced form of botnet that exploits a Domain Generation Algorithm (DGA) to generate seemingly random domain names for its command and control (C&C) infrastructure, such as Mirai [18] and other well-known botnets listed on [Netlab 360](#). The primary objective of using a DGA is to create difficulties for security researchers and law enforcement agencies in tracking and dismantling the botnet's C&C servers, as the generated domain names change regularly. Cybercriminals commonly employ DGA-based botnets to carry out various malicious activities, including spamming, distributing malware, launching DDoS attacks, and stealing data [17]. These botnets have the ability to infect numerous computers and devices, forming a network that serves various illicit purposes. Compared to other types of botnets, DGA-based botnets are known for their resilience and the challenge they pose in terms of tracking and blocking, as they continuously alter their C&C infrastructure, making it

more arduous to disrupt their operations [19]. The objective of this paper is to evaluate the current capabilities of Noisy Intermediate-Scale Quantum (NISQ) hardware [20] using a hybrid quantum machine learning approach to detect DGA botnets, and to explore how quantum machine learning (QML) can enhance the functionality of Security Information and Event Management (SIEM), and Security Orchestration, Automation, and Response (SOAR) systems.

2.2. Machine Learning. Machine learning is a branch of artificial intelligence (AI) that enables software applications to predict outcomes more accurately without the need for explicit programming [2]. Machine learning algorithms use historical data to predict new output values. This allows them to learn from data and improve their performance over time. It is thus a natural choice to consider machine learning to detect botnets by analyzing network traffic data.

There are various approaches to implementing machine learning, one of which is supervised classification applied to network traffic data. Brezo et al. proposed a supervised classification method for detecting malicious botnet traffic by analyzing network packets [21]. Piras, Pintor, Demetrio, and Biggio explored techniques for explaining Machine Learning DGA detectors using DNS traffic data and benchmarked different models, including J48 Decision Tree, k-nearest Neighbors, and Random Forest [22]. Jia, N. Wang, Y.-Y. Wang, and Hu analyzed the traceability and reconstructed the attack path of a botnet control center using an ant colony group-dividing algorithm [23]. Pérez et al. introduced an approach for proactive detection and mitigation of botnets in 5G Mobile Networks, utilizing software-defined network and network function virtualization techniques [24]. Onotu, Day, and Rodrigues demonstrated how Neural Nets can recognize shellcode from network traffic data by employing a multi-layer perceptron approach with a back-propagation learning algorithm [25]. Maniriho, Mahmood, and Chowdhury conducted a survey on malware detection and classification techniques, considering botnets as a subset of malware from a classical computing perspective [26].

In conclusion, machine learning offers a powerful way to detect botnets. However, challenges that remain are performance degradation over time of ML algorithms as botnets evolve and change their tactics, but also the fact that ML algorithms are susceptible to adversarial attacks. Adversarial attacks are designed to fool ML algorithms into making incorrect predictions. This can be done by injecting malicious traffic into a network that is designed to look like benign traffic. For the purposes of this work, the use of ML for botnet detection gives us a good benchmark to compare and ground our experimentation with quantum machine learning.

2.3. Hybrid Quantum Machine Learning. Hybrid Quantum Machine Learning (HQML) is an innovative approach that combines the power of quantum computing

and classical machine learning. HQML algorithms utilize both quantum and classical computers to tackle complex problems that go beyond the capabilities of either technology alone [27]. Researchers propose two types of hybridization to achieve quantum advantage: vertical hybridization, which involves leveraging quantum devices with a hardware-agnostic low-level design, topology mapping, and error correction routines; and horizontal hybridization, which divides an algorithm into pre-processing, quantum circuit involvement, and post-processing stages to attain quantum advantage through a software-based approach [28]. In the domain of Quantum Cybersecurity Analytics (QCA), Hybrid Quantum Binary Classifiers (HQBC) can be employed to detect various adversarial cyber events, including spam, phishing, spyware, ransomware, and botnets. In this paper, we demonstrate that Hoeffding Trees outperform classical machine learning binary classifiers and all known quantum approaches in detecting Domain Generation Algorithm (DGA) botnets. Furthermore, we investigate the conditions under which HQBCs can achieve comparable or superior performance compared to classical machine learning models in DGA botnet detection.

As a related work exploring the application of HQML for DGA botnet detection, [12] investigates Hybrid Quantum Deep Learning (HQDL) and Variational Quantum Classifier (VQC) approaches using the IBM quantum infrastructure based on superconducting loops-hardware. The authors simulate the performance of different combinations of key optimizers with variational forms and feature maps. The robustness of HQDL models against adversarial attacks is also examined [29]. The results reveal that a hardened version of the HQDL model can withstand adversarial attacks. This study on HQML for DGA botnet detection [12] highlights several knowledge gaps that need to be addressed:

- (1) How do other quantum supervised-learning methods perform in detecting DGA botnets?
- (2) What is the impact of different qubit approaches, such as trapped ions, silicon quantum dots, topological qubits, and diamond vacancies, on performance and hardware design?
- (3) How does the time complexity of different architectural elements influence performance?

This article focuses specifically on the first knowledge gap. In particular, we will evaluate existing HQBCs that play a crucial role in cybersecurity decision systems, including spam detection, anomaly detection, and botnet detection, among others.

2.4. Quantum Machine Learning. Researchers have recently investigated a novel approach to intrusion detection by employing quantum machine learning (QML) algorithms [30]. The study conducted experiments to demonstrate the effectiveness of QML-based intrusion detection in processing large-scale data inputs with remarkable

accuracy (98%). Notably, the QML approach exhibited twice the speed compared to conventional machine learning algorithms typically used for the same task. These findings highlight the potential of QML approaches to surpass the performance of classical methods in intrusion detection, showcasing their promising capabilities in the field.

3. METHODOLOGY

The methodology section emphasizes the experimental decisions made in this research. The first Subsection 3.1 covers the selection of quantum devices, real-device-based simulators, and quantum simulators utilized for conducting the experiments. The second Subsection 3.2 provides an explanation for the selection of the IEEE Botnet DGA Dataset, justifying its suitability for the analysis conducted in this research.

3.1. Selected Platforms. For this research, we opted to use a combination of real quantum devices, real-device-based simulators, and quantum simulators (pure software-based emulators) to reproduce the results reported in the study by Suryotrisongko et al. [31], which focused exclusively on quantum simulators. Additionally, our experiments were conducted on three Azure Quantum Providers to expand the research scope beyond the utilization of IBM Quantum [31]. The real quantum devices we selected for our experiments were IonQ, Rigetti, and Quantinuum. To perform quantum simulations, we relied on the Qiskit SDK, utilizing Aer for simulations and real-device-based simulations.

The quantum computing configurations used in our experiments are presented in Table 1. The first column introduces a naming convention for referencing the platforms, facilitating better comprehension of the experimental results presented in Section 5. Platforms functioning as real quantum devices are denoted by their respective names followed by the letter R. Platforms that combine real quantum devices with simulations, thereby serving as real-device-based simulators, are denoted by their names followed by the letter S.

3.2. Description of the Dataset. In this study, we evaluated our findings on DGA botnets using two datasets: the IEEE Botnet DGA Dataset [31, 32] and the UMUDGA dataset [33]. The UMUDGA dataset consists of 50 malware samples and is suitable for multiple classifications using HQBCs. However, for the purpose of comparing our results to [12], we focused solely on the IEEE Botnet DGA Dataset in the current experiments. Nonetheless, the UMUDGA dataset may be considered for future investigations.

The IEEE Botnet DGA Dataset comprises a total of 1,803,333 data records. For our experiments, we randomly selected data samples from this dataset. Specifically, we used 1,000 fixed random data samples for quantum simulators, following the approach in [12], and real-device-based simulators. Additionally, we utilized 100 fixed random

Naming Convention	Machine Name	Device Mode
Aer	Qiskit	Quantum simulator
Quantinuum-R	Quantinuum H1-2	Real quantum device
Quantinuum-S	Quantinuum H1-2 Emulator	Real-device-based simulator
Rigetti-R	Rigetti Aspen-M-3 with Qiskit	Real quantum device
Rigetti-S	Rigetti QVM	Real-device-based simulator
IonQ-R	IonQ Aria	Real quantum device
IonQ-R	IonQ Quantum Simulator	Real-device-based simulator

TABLE 1. Naming conventions for selected platforms shown with their machine name and their device mode (quantum simulator, real-device-based simulator, or real quantum device)

data samples for real quantum devices, and a separate set of 5,000 fixed random data samples to test the new algorithm on real-device-based simulators.

As described in [12], we extracted seven features from the analyzed domain names in the dataset. These features include:

- (1) CharLength: The character length of the domain name.
- (2) EntropyValue: The entropy value calculated using Shannon’s function with the probability distribution of characters in the domain name.
- (3) RelativeEntropy: The distance or similarity of a domain name to the character probability distributions of either Alexa or DGA domain names, measured using the Kullback-Leibler divergence function.
- (4) MinREBotnets: The minimum relative entropy with the domain names of DGA botnets.
- (5) InformationRadius: The similarity or distance of a domain name to the domains of the ten botnet DGA families, calculated using the Jensen-Shannon divergence function.
- (6) TreeNewFeature: A feature generated by a decision tree algorithm that combines the features Entropy, REAlexa, MinREBotnets, and CharLength to train a predictive model.
- (7) Reputation: Provides information about the popularity and credibility of the website.

The summarized statistics for these features, including the mean, standard deviation, minimum, median, maximum, skewness, and kurtosis values, are presented in Table 2.

Feature	Mean	StDev	Min.	Median	Max.	Skewness	Kurtosis
CharLength	17.20	6.82	4.00	16.00	73.00	0.81	0.02
EntropyValue	3.02	0.53	0.00	3.04	4.78	-0.40	0.83
RelativeEntropy	1.66	0.82	0.20	1.55	10.10	1.63	6.91
MinREBotnets	1.28	0.57	0.00	1.23	5.99	0.84	1.24
InformationRadius	0.65	0.11	0.24	0.65	1.17	0.34	0.12
TreeNewFeature	0.45	0.34	0.00	0.35	0.99	0.38	-1.52
Reputation	81.66	54.12	0.00	64.51	436.31	0.99	0.21

TABLE 2. Selected descriptive statistics of the IEEE Botnet DGA Dataset [31] for the seven features according to the Anderson-Darling normality test.

4. STABLE ARCHITECTURE FOR LONG-RUNNING EXPERIMENTS

This section discusses the issues encountered during long-running experiments and presents a stabilized architecture to address these problems. It includes the introduction of a new binary classifier and highlights relevant implementation issues.

4.1. Reasons for Instability. The current versions of Qiskit ML classifiers (qiskit-0.41.1 and qiskit-machine-learning-0.5.0), specifically QSVC, Pegasos, VQC, and QNN, have not been tested for compatibility with Azure Quantum Providers such as IonQ, Rigetti, and Quantinuum. Additionally, graceful exception handling has not been implemented. As a result, during the experimentation phase, we frequently experienced instability, including unexpected aborts and missing error messages in long-running notebook sessions. Code hardening revealed the following reasons for instability during experiments on real quantum devices:

- (1) Issues on the real quantum devices
 - (a) Failure of a single circuit run causing a cascade effect regardless of progress.
 - (b) Prioritization and scheduling bugs in the task queue.
 - (c) Maintenance downtime.
 - (d) Inability to deploy the quantum cloud architecture on a small scale due to insufficient or outdated documentation.
- (2) Issues with the hosted Jupyter notebooks in Azure Quantum workspace
 - (a) Kernel failure.
 - (b) Low memory.
 - (c) Insufficient number of virtual CPUs.
 - (d) Lack of visibility on progress and log processing.
- (3) Issues in the communication between real quantum devices and notebooks

- (a) Authentication and session failures.
- (4) Issues with the Jupyter Notebook on the client side
 - (a) Termination after a maximum of 24 hours, regardless of CPU or RAM power.
- (5) Issues related to different real devices
 - (a) Deprecated APIs of Qiskit.
- (6) Issues stemming from the nature of the algorithm
 - (a) Excessive number of loops.
 - (b) Lack of code portability.
 - (c) Inadequate exception handling.

LIST 1. Reasons for instability

We discovered that the stability of computing and network elements within the architecture is the primary limitation of cloud-based quantum computer delivery. However, none of our experiments on real quantum devices could last longer than three weeks. We were unable to establish a stable TLS connection and authentication for a 1,000 random fixed data sample, leading us to select a reduced sample size of 100 random fixed data points for real quantum devices.

Subsection 4.2 will present an architecture design that addresses points (1)-(5) in List 1 of instability reasons. Furthermore, Subsection 4.3 will discuss necessary algorithmic changes to tackle point (6) in List 1. It is important to note that our experiments running on quantum simulators did not exhibit any instability.

4.2. Stabilized Architecture. Our enhanced architecture design addresses the instability reasons (1)-(5) in List 1. The original architecture that led to instabilities consisted of an Azure real quantum device and an Azure component that involves an Azure Job Management, a storage account and a authentication component.

The updated architectures introduce additional components to solve the instability issues mentioned in List 1. Experiments except QHTC are build on the architecture displayed in figure 1 and QHTC experiments apply the architecture in figure 2.

The architecture for experiments except QHTC includes a preceding step in a Google Cloud instance, where a Jupyter and Google Colab Notebook can be deployed on dedicated virtual machines to enable longer runtimes beyond the 24-hour limit. The additional Jupyter Notebook facilitates the implementation of Qiskit code changes for exception handling specific to the algorithm and real quantum device. The Google Colab Pro+ Notebook provides stable runs for more than 1000 random fixed data samples. Additionally, a monitoring instance of a GCP virtual machine with diverse logging capabilities aids in identifying, tracking, and resolving errors, including authentication and session failures.

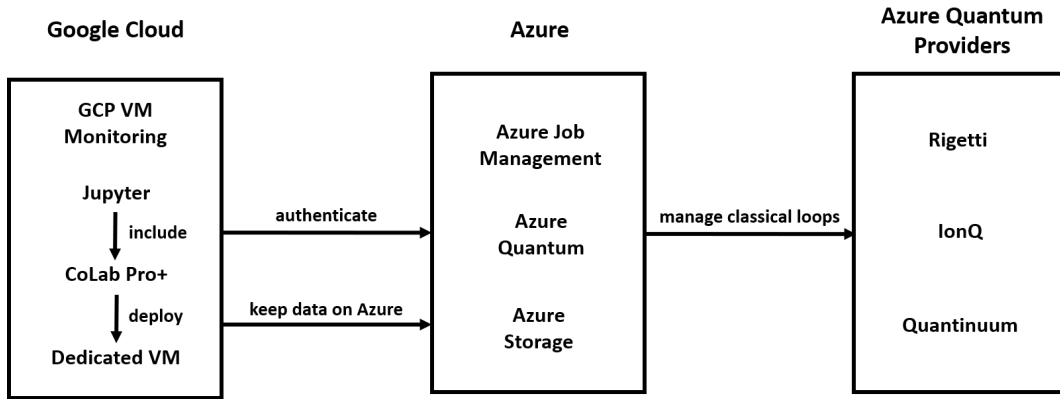
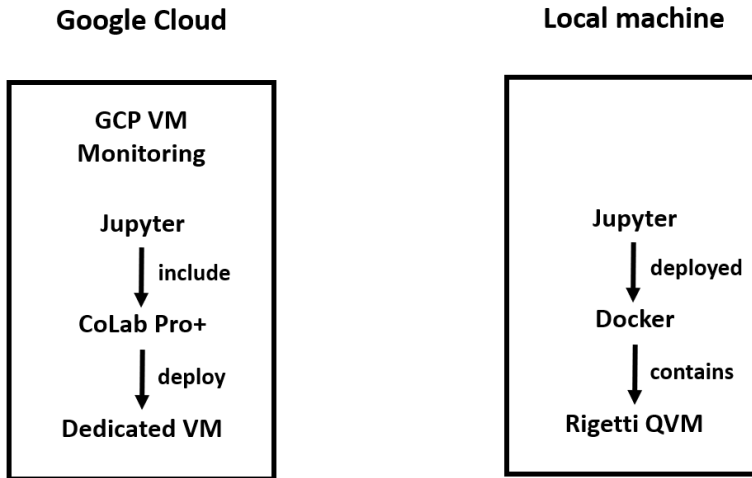


FIGURE 1. Stabilized architecture of experiments on real quantum devices comprising of three components Google Cloud, Azure and Azure Quantum Providers.



(a) Stabilized architecture for QHTC experiment on Aer

(b) Stabilized architecture for QHTC experiments on Rigetti-S

FIGURE 2. Stabilized architecture for QHTC experiments on quantum simulators Aer and Rigetti-S. The difference in implementation originates from differences in library functionalities available on Aer and Rigetti-S.

HQML (Hybrid Quantum Machine Learning) opens the door to a new generation of Security Information and Event Management systems known as quantum-enhanced SIEM (QSIEM). To illustrate the functioning of a QSIEM, we present the first use case: defending against Domain Generation Algorithm (DGA) Botnet attacks for DDoS at the application layer using a quantum-enhanced SIEM. The integration of HQML with a robust SIEM like Azure Sentinel becomes highly beneficial at OSI-layer 7 (application layer), where HTTP and DNS traffic occur. This integration enables the detection of malicious domain names generated by DGA-Botnets for command-and-control servers, which are crucial for coordinating DDoS attacks. By identifying and blocking traffic associated with these domains, botnets can be prevented from receiving commands or initiating attack traffic.

Our stabilized architecture aligns with the concept of a quantum-enhanced SIEM solution. The steps in Figure 3 are explained in List 2. Steps (2)-(9) are specific to training the HQML algorithm, while the productive algorithm utilizes telemetry input data to generate a classification using Quantum SIEM and Azure Sentinel, which is then displayed on the dashboard.

- (1) Gather and preprocess the telemetry data required for the algorithm described in Subsection 4.3.
- (2) Perform classic feature engineering as described in Subsection 3.2.
- (3) Deploy the algorithm for production use on Azure Quantum service.
- (4)-(7) Execute the entire circuit to and from the real quantum devices using the classical loop.
- (8) Collect all the results and accumulate the final output.
- (9) Save and update the classification algorithm.
- (10) Integrate the classification algorithm with Azure Sentinel.
- (11) Display the results of the classification algorithm to the user.

LIST 2. Steps in the solution architecture

4.3. Quantum-enhanced Hoeffding Tree Classifier (QHTC). This subsection first describes the historical development of our scientific advances in the direction of the solution, followed by an explanation of the quantum-enhanced Hoeffding Tree Classifier (QHTC).

A realistic QCA solution, i.e., the quantum-enhanced SIEM in 4.2, needs to be able to process online big data streaming. Hence, we sought an incremental approach to be applied to already known HQBCs. The most promising algorithmic candidate to reduce execution time and improve accuracy when executed on real-device-based simulators was the PegasosQSVC, in our opinion. Due to its stochastic gradient descent optimizer, the PegasosQSVC performs fewer calculations by iterations and results in

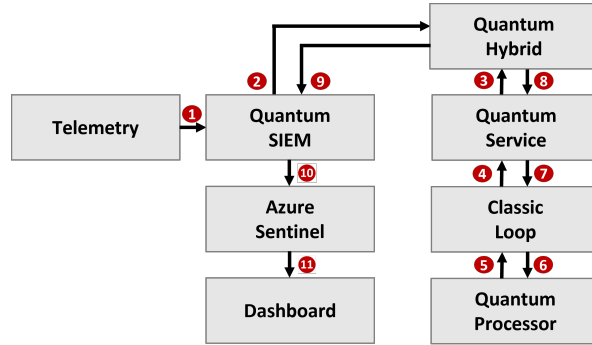


FIGURE 3. Quantum-enhanced SIEM. The individual steps are marked with numbers in red circles and are explained in List 2

better generalization properties of the trained model than conventional gradient descent [34]. Instead of making the PegasusQSVC truly incremental, we applied a batch-wise strategy as an intermediate step between algorithms that need to process the entire training or test data samples at once and incremental algorithms.

The performance of PegasusQSVC with respect to accuracy development over time is displayed in Figure 4 for batch sizes of 1,000 as well as 100 random fixed data samples on the quantum simulator Aer. The PegasusQSVC shows good behavior in terms of accuracy increase with the number of batches if a batch size of 1,000 data samples per batch is applied. But the real quantum devices are not able to handle 1,000 data samples, but only 100 data samples per batch, as the results in Subsection 5.1 will show. In contrast, a batch size of 100 samples will not exhibit the appropriate increase in accuracy on real-device-based simulators or real quantum devices. Smaller batch sizes in the range of 100 data samples require a higher number (one magnitude) of circuits to be sent to the real quantum device, which will extend the execution time to an inappropriate level. This is the dilemma of NISQ-limited data volumes.

Therefore, we decided to transition to a truly incremental algorithm and apply it batch-wise to reduce the number of shots sent to the real quantum device. The accuracy of a truly incremental algorithm will not suffer in this way. This was the breakthrough in terms of the algorithm’s accuracy and execution time on real-device-based simulators.

We found the algorithmic solution in a quantum-modified version of an incremental decision tree approach called the Hoeffding tree algorithm [35], shown in algorithm 1. It is a generation algorithm for incremental decision trees that applies the Hoeffding bound [36, 37]. The standard non-incremental version of the decision tree takes all data samples per leaf at once to compute a decision criterion per leaf. In contrast, the incremental version of a decision tree can process one data sample after another.

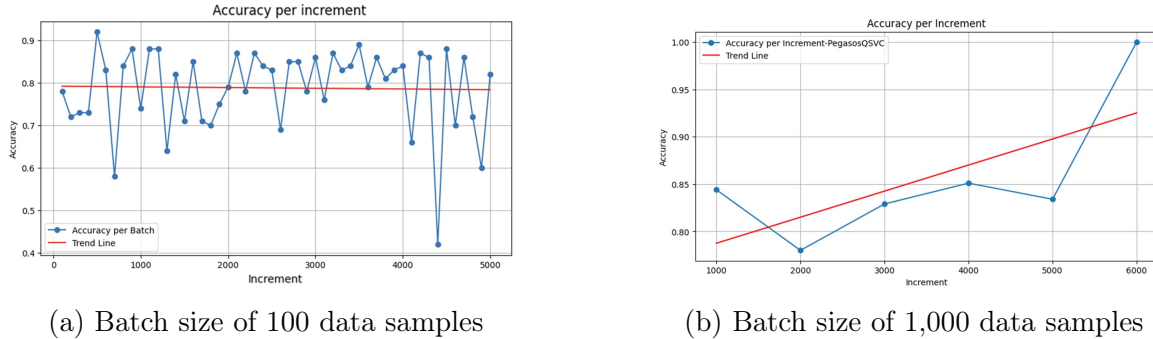


FIGURE 4. PegasosQSVC’s accuracy on quantum simulator AER with (a) a batch size of 100 data samples does not improve its accuracy with an increased number of batches, unlike (b) a batch size of 1,000 data samples.

The main advantage of this generation algorithm is that it guarantees, under realistic assumptions, the generation of an asymptotically arbitrarily similar incremental version of a decision tree compared to the same non-incremental version of the decision tree. Simultaneously, it maintains efficient computation speed. Additionally, the Hoeffding bound is independent of the probability distribution of the data samples. However, this implies the disadvantage that the Hoeffding bound, compared to distribution-dependent bounds, requires more data samples to reach the same level of similarity between the incremental version and non-incremental version of the decision tree.

We introduce the abbreviation HTC (Hoeffding Tree Classifier) for the original Hoeffding tree, shown in algorithm 1. Our quantum-modified version is called the quantum-enhanced Hoeffding Tree Classifier (QHTC), as presented in algorithm 4 and described below. QHTC is a batch-wise learning procedure that applies HTC with modified input data. We apply the HTC in an equivalent version following the HTC implementation of [38] that is shown in algorithms 2 and 3. The first step of QHTC is the mapping of the classical features of the input data to the quantum feature space using ZFeatureMap, although other mappings are also possible. Each feature column entry in the feature row represents a data point in quantum space (qubit) on the Bloch sphere and we want to measure the length of the cycle connecting all qubits per feature row. The reason is that the distance between two qubits represents a measure of how distinguishable they are. This cycle length is referred to as a ‘quantum walk’ in the code.

The measurement of the cycle length relies on measuring the distance between two qubits on the Bloch sphere. For that, each qubit is converted via wave functions to its density matrix. These density matrices are listed in the same order as the classical

feature columns and the trace distance of two density matrices is applied to measure the distance between two qubits that are neighbors on the cycle.

The cycle length is determined by the order of data points in quantum space and, hence, by the order of the classical features given in the original data set. The determination of a distance metric that allows reordering of feature columns is left for future research. The initialization of HTC is performed accordingly.

The batch-wise computation of an incremental decision tree reduces the number of shots sent to the real quantum device drastically compared to usual loop-based optimizers, while not compromising its accuracy. This provides a solution to the instability reason (6a) mentioned in List 1. It allows us to deal with the realistic behavior of today’s real quantum devices that are prone to instability due to the noise problem inherent in today’s NISQ devices. The execution times and the accuracy benefit accordingly, as the results in Section 5 show in more detail.

5. EXPERIMENTAL RESULTS

The experimental results for different algorithms and quantum devices are presented in the following subsections, focusing on execution time, accuracy, and additional performance metrics for the QHTC algorithm.

5.1. Execution Time and Accuracy. In this section, we present the experimental results for different binary classifiers, including VQC, PegasosQSVC, QSVC, SamplerQNN, and EstimatorQNN, in terms of accuracy and execution time on quantum simulators, real-device-based simulators, and real quantum devices.

Tables 3 and 4 showcase the accuracy, total computation time (T_{total}), chosen feature map, and optimizer for various combinations of platforms and algorithms. The experiments on quantum simulators and real-device-based simulators were conducted with at least 1,000 random fixed data samples, while the experiments on real quantum devices used 100 data samples due to computational limitations and instabilities.

On real quantum devices, the PegasosQSVC performs well in terms of execution time due to its SGD optimizer which tends to converge a little faster than non stochastic optimizers. The PegasosQSVC stands out as the superior binary classifier. As the APIs of feature maps of Qiskit (see for example [ZFeatureMap](#)) have no endpoint to change the quantum real device, specific implementations are needed for each algorithm. Hence, we didn’t intend to compare QHTC over different quantum real devices. We left the implementation of additional coding routines in order to enforce specific real quantum devices and real-device-based simulators for future investigations.

The PegasosQSVC shows good accuracy (90%) and very good execution time (45 seconds) on real-device-based simulators. However, the QHTC algorithm outperforms all other binary classifiers in terms of accuracy, achieving perfect accuracy of 100%

Algorithm and Platform	FeatureMap	Optimizer	Accuracy [%]	T_{total} [s]
VQC-IonQ-R	ZFeatureMap	COBLYA	50	1,325,133
PegasosQSVC-IonQ-R	ZFeatureMap	SGD	41	156,156
QSVC-IonQ-R	ZFeatureMap	COBLYA	53	283,325
SamplerQNN-IonQ-R	ZFeatureMap	COBLYA	56	956,540
EstimatorQNN-IonQ-R	ZFeatureMap	COBLYA	59	1,165,819
VQC-Rigetti-R	ZFeatureMap	COBLYA	43	1,176,879
PegasosQSVC-Rigetti-R	ZFeatureMap	SGD	48	355,509
QSVC-Rigetti-R	ZFeatureMap	COBLYA	39	385,153
SamplerQNN-Rigetti-R	ZFeatureMap	COBLYA	53	1,601,895
EstimatorQNN-Rigetti-R	ZFeatureMap	COBLYA	51	1,437,085
VQC-Quantinuum-R	ZFeatureMap	COBLYA	44	972,732
PegasosQSVC-Quantinuum-R	ZFeatureMap	SGD	44	972,732
QSVC-Quantinuum-R	ZFeatureMap	COBLYA	45	472,847
SamplerQNN-Quantinuum-R	ZFeatureMap	COBLYA	46	1,087,789
EstimatorQNN-Quantinuum-R	ZFeatureMap	COBLYA	50	1,167,143

TABLE 3. Performance results in terms of accuracy and total execution time T_{total} of real quantum devices, using 100 data samples for all runs. For each algorithm and platform, the choice of the feature map and the optimizer is also shown.

already after 3 out of 5 batches. The accuracy is discussed in more detail in subsection 5.2. Furthermore, QHTC exhibits significantly reduced total execution time compared to other algorithms on real-device-based simulators.

The experiments conducted on real-device-based simulators and real quantum devices considered a first step, and further improvements and specific implementations for each algorithm on different devices can be explored in future research. Overall, these results demonstrate that it is possible to construct superior algorithms for cloud-based NISQ deployments on real-device-based simulator Rigetti, achieving comparable execution times to quantum simulators while exceeding in terms of accuracy.

5.2. Performance Metrics of QHTC. We show the results of our QHTC (see algorithm 4) which is configured to run with five batches containing 1,000 random fixed data samples each. We apply the feature map ZFeatureMap provided by Qiskit. Table 5 demonstrates achievements in terms of accuracy improvement. The increase in accuracy with the number of batches meets our expectations. QHTC yields the same results for all three feature maps. We obtained an average accuracy of 91.2% and a

Algorithm and Platform	FeatureMap	Optimizer	Accuracy [%]	T _{total} [s]
VQC-Aer	ZZFeatureMap	COBYLA	54	4,240
PegasosQSVC-Aer	ZFeatureMap	SGD	90	45
QSVC-Aer	ZFeatureMap	COBYLA	87	3,091
SamplerQNN-Aer	ZFeatureMap	COBYLA	76	374
EstimatorQNN-Aer	ZFeatureMap	COBYLA	84	410
VQC-IonQ-S	ZFeatureMap	COBYLA	51	957,755
PegasosQSVC-IonQ-S	ZFeatureMap	SGD	49	113,950
QSVC-IonQ-S	ZFeatureMap	COBYLA	50	178,529
SamplerQNN-IonQ-S	ZFeatureMap	COBYLA	59	746,992
EstimatorQNN-IonQ-S	ZFeatureMap	COBYLA	63	780,480
VQC-Rigetti-S	ZFeatureMap	COBYLA	46	889,708
PegasosQSVC-Rigetti-S	ZFeatureMap	SGD	55	206,729
QSVC-Rigetti-S	ZFeatureMap	COBYLA	45	205,877
SamplerQNN-Rigetti-S	ZFeatureMap	COBYLA	58	656,629
EstimatorQNN-Rigetti-S	ZFeatureMap	COBYLA	54	955,654
VQC-Quantinuum-S	ZFeatureMap	COBYLA	45	806,626
PegasosQSVC-Quantinuum-S	ZFeatureMap	SGD	49	174,416
QSVC-Quantinuum-S	ZFeatureMap	COBYLA	49	197,871
SamplerQNN-Quantinuum-S	ZFeatureMap	COBYLA	48	852,774
EstimatorQNN-Quantinuum-S	ZFeatureMap	COBYLA	53	716,581
QHTC-Rigetti-S	ZFeatureMap	n.a.	100 ^a	1,687

^aAlready after 3 out of 5 batches

TABLE 4. Performance results in terms of accuracy and total execution time T_{total} of quantum simulator and real-device-based simulator experiments, using 5,000 data samples for QHTC, and 1,000 data samples for all other algorithms. For each algorithm and platform, the choice of the feature map and the optimizer is also shown.

final-round accuracy of 100% for QHTC already after 3 out of 5 batches. We used the same features and the same dataset as [12] to be able to compare our results with theirs. These features are the same features that are available in the entire dataset itself. This may be the reason for such high accuracy. In future research, we can further improve the metric computation to avoid over-fitting and to make it more realistic by applying a PCA analysis as well as using a k-fold cross-validation per batch, with $k = 10$ for example. In addition, the features EntropyValue and RelativeEntropy possess strong

predictor properties for the entire dataset. Hence, the same issue will probably not happen to other datasets that don't possess very strong predictor features.

Batch	Accuracy [%]	F1-score [%]	AUC [%]
1	57.1	4.5	51.1
2	99.0	98.8	98.9
3	100.0	100.0	100.0
4	100.0	100.0	100.0
5	100.0	100.0	100.0
Average	91.2	80.7	90.0

TABLE 5. Metric results in terms of accuracy, F1-score and AUC for algorithm QHTC, displayed for 5 batches with 1,000 data samples each and their average.

6. CONCLUSION AND FUTURE WORK

Cybersecurity Analytics involves the collection of data to gather evidence, construct timelines, and analyze threats, thereby enabling the design and execution of a proactive cybersecurity strategy that detects, analyzes, and mitigates cyber threats. The next-generation Quantum Cybersecurity Analytics utilizes hybrid quantum machine learning (HQML) to monitor network activity, promptly identify resource use or network traffic changes, and address threats. This advancement paves the way for a new generation of Security Information and Event Management systems called quantum-enhanced SIEM (QSIEM). To illustrate how a QSIEM operates, we presented the first use case of defending against DGA botnet attacks for DDoS at the application layer using a quantum-enhanced SIEM.

As cybersecurity is built upon the analysis of amounts of big data, today's NISQ era poses an obstacle for quantum-enhanced SIEM for cybersecurity due to its inherent instabilities that enlarge with repeated and prolonged computations. This study found a way to overcome parts of the problem by proposing a new form of HQML binary classifiers that lead to significant improvements in the result's accuracy as well as the algorithm's execution times with real-device-based simulations compared to previous algorithms. The breakthrough was the application of a quantum-enhanced version of the incremental Hoeffding tree algorithm in a batch-wise version in order to take account of large amounts of incoming online stream data in addition to responding to the need for a reduced number of shots to the real quantum device. In addition to the improved accuracy, the experimental run times in real-device-based simulations were

reduced drastically by three orders of magnitude to be in the same order as with the previous algorithms on the quantum simulator Aer that is deployed locally.

In general, the world of quantum simulators is much more beautiful than the world of computations on real quantum devices. This study showed for the first time that HQML algorithms were able to run stably with 100 random fixed data samples for several weeks on Azure Quantum Providers Rigetti, Quantinuum, and IonQ together with the library Qiskit. It is the first time these tools were combined. We achieved this by code hardening throughout the entire data flow process from the Jupyter Notebook to the real quantum devices, including all communications and algorithm-specific implementations of APIs per real quantum device. However, future research needs to build upon our progress in order to make the quantum computations on real devices stable for a much larger portion than 100 random fixed data samples, being just a very small fraction of the entire IEEE Botnet DGA Dataset. The enlargement of stability may also be pursued in the case of quantum simulations, as we only used a random fixed sample size of 1,000 in the usual HQBC case and a random fixed sample size in the QHTC case when conducting real-device-based simulations.

Moreover, we left the implementation of additional coding routines in order to enforce all specific real quantum devices or real-device-based simulators in the case of the quantum-enhanced version as well as the original version of the Hoeffding tree algorithm for future investigations. In addition, the determination of a distance metric for QHTC that allows reordering of feature columns is left for future research. Our focus of this study in this regard was to show the excellent properties of these HQBC algorithms for the DGA botnet classification problem in which we succeeded.

For future research, we also suggest investing more into PegasosQSVC because if we combine quantum supervised learning with rewarding and quantum reinforcement learning, we may have groundbreaking cybersecurity tools. Because current NISQ and hybrid models can support up to 5,600 qubits, perhaps we don't have a 5,600 network feature in cyber data. Resulting from that, even in this NISQ period, we can probably make strong cyber use cases for existing quantum computers and HQML.

Furthermore, it is an open question as to what practical problem of which scientific fields the same approach of quantum-enhanced Hoeffding tree algorithms might apply as well. The UMUDGA dataset may be a next suitable choice for the DGA botnet detection field. We elaborated on a number of features of the IEEE Botnet DGA Dataset in order to give researchers from other fields a good starting point for their investigations.

Acknowledgements. We acknowledge support from Microsoft's Azure Quantum for

providing credits and access to the IonQ, Quantinuum and Rigetti systems used in this paper.

APPENDIX A. PSEUDO-CODE ALGORITHMS

Algorithm 1 The Original Hoeffding Tree Algorithm [35] (HTC)

Inputs:

- S is a sequence of examples.
- \mathbf{X} is a set of discrete attributes.
- $G(\cdot)$ is a split evaluation function.
- δ is one minus the desired probability of choosing the correct attribute at any given node.

Output:

- HT is a decision tree.

```

1: procedure HoeffdingTree( $S, \mathbf{X}, G, \delta$ )
2:   Let  $HT$  be a tree with a single leaf  $l_1$  (the root).
3:   Let  $\mathbf{X}_1 = \mathbf{X} \cup \{X_\emptyset\}$ .
4:   Let  $\bar{G}_1(X_\emptyset)$  be the  $\bar{G}$  obtained by predicting the most frequent class in  $S$ .
5:   for each class  $y_k$  do
6:     for each value  $x_{ij}$  of each attribute  $X_i \in \mathbf{X}$  do
7:       Let  $n_{ijk}(l_1) = 0$ .
8:     end for
9:   end for
10:  for each example  $(\mathbf{x}, y_k)$  in  $S$  do
11:    Sort  $(\mathbf{x}, y)$  into a leaf  $l$  using  $HT$ .
12:    for each  $x_{ij}$  in  $\mathbf{x}$  such that  $X_i \in \mathbf{X}_l$  do
13:      Increment  $n_{ijk}(l)$ .
14:    end for
15:    Label  $l$  with the majority class among the examples seen so far at  $l$ .
16:    if the examples seen so far at  $l$  are not all of the same class then
17:      for each attribute  $X_i \in \mathbf{X}_l - \{X_\emptyset\}$  do
18:        Compute  $\bar{G}_l(X_i)$  using the counts  $n_{ijk}(l)$ .
19:      end for
20:      Let  $X_a$  be the attribute with the highest  $\bar{G}_l$ .
21:      Let  $X_b$  be the attribute with the second-highest  $\bar{G}_l$ .
22:      Compute  $\epsilon = \sqrt{\frac{R^2}{2} \cdot \ln\left(\frac{1}{\delta}\right) \cdot \frac{1}{\sum_{ijk} n_{ijk}(l)}}$ .
23:      if  $\bar{G}_l(X_a) - \bar{G}_l(X_b) > \epsilon$  and  $X_a \neq X_\emptyset$  then
24:        Replace  $l$  by an internal node that splits on  $X_a$ .
25:        for each branch of the split do
26:          Add a new leaf  $l_m$ , and let  $\mathbf{X}_m = \mathbf{X} - \{X_a\}$ .
27:          Let  $\bar{G}_m(X_\emptyset)$  be the  $\bar{G}$  obtained by predicting the most frequent class at  $l_m$ .
28:          for each class  $y_k$  and each value  $x_{ij}$  of each attribute  $X_i \in \mathbf{X}_m - \{X_\emptyset\}$  do
29:            Let  $n_{ijk}(l_m) = 0$ .
30:          end for
31:        end for
32:      end if
33:    end if
34:  end for
35:  return  $HT$ .
36: end procedure

```

Algorithm 2 The HoeffdingTreeClassifier (HTC) following implementation [38]

```

1: procedure INIT( $nFeatures$ ,  $nClasses$ ,  $delta = 0.01$ ,  $tiethreshold = 0.05$ )
2:   Store the input variables.
3:    $root \leftarrow \text{TREENODE}(delta)$ 
4: end procedure

5: function PREDICT( $X$ )
6:   Predict the class labels for the input instances  $X$ .
7:   return  $yPredict$ 
8: end function

9: procedure PARTIALFIT( $X$ ,  $y$ )
10:  Update the tree with new training instances  $X$  and their corresponding class labels  $y$ .
11: end procedure

12: procedure UPDATESTATISTICS( $X$ ,  $label$ )
13:  Update the statistics of the tree nodes based on the input instance  $X$  and its class label  $label$ .
14: end procedure

15: procedure ATTEMPTSPLIT( $node$ )
16:  Attempt to split the given node  $node$  based on the Hoeffding bound gain.
17: end procedure

18: procedure SPLITNODE( $node$ )
19:  Split the given node  $node$  by selecting the best attribute based on the Hoeffding bound gain.
20: end procedure

21: function HoeffdingBOUND( $node$ )
22:  Split the given node  $node$  by selecting the best attribute based on the Hoeffding bound gain.
23:  return  $epsilon$ 
24: end function

```

Algorithm 3 TreeNode (as part of algorithm 2)

```

1: procedure INIT(delta)
2:   Store the input variable.
3:   Initialize further variables.
4: end procedure

5: function ISLEAF
6:   Check if the node is a leaf (no children).
7:   return not children
8: end function

9: procedure COMPUTEERRORRATE
10:  Compute the error rate of the node based on the class distribution.
11: end procedure

12: procedure COMPUTEBESTSPLITTINGATTRIBUTE(nClasses, nFeatures)
13:  Compute the best attribute to split on based on the Hoeffding bound gain.
14: end procedure

15: function COMPUTEHOEFFDINGBOUNDGAIN(classCountsPerValues, totalSamplesPerValue, nClasses,
    totalSamples)
16:  Compute the Hoeffding bound gain for the given attribute values and their class counts.
17:  return gain
18: end function

19: function HOEFFDINGBOUND(errorRate)
20:  Compute the Hoeffding bound for the given error rate errorRate.
21:  return hoefdingBound
22: end function

23: function GETMAJORITYCLASS
24:  Get the majority class label based on the class distribution.
25:  return majorityClass
26: end function

```

Algorithm 4 Batch-wise Learning with the Quantum-enhanced Hoeffding Tree Classifier (QHTC)

```

1: procedure RUNQHTC
2:   Load the data set.
3:   Extract the features and labels from the data set.
4:   Normalize the features using a standard scaler.
5:   Initialize a few variables.
6:   for each feature row  $r$  in data set do
7:     Compute quantum walk distance QHTCDISTANCERIGETTI( $r$ ).
8:   end for
9:   Store the new quantum data rows as a combination of the quantum walk distances and labels.
10:  Initialize number of features  $nFeatures$  with 1.
11:  Initialize number of classes  $nClasses$  with number of unique values in labels.
12:  Initialize function HoeffdingTree.INIT( $nFeatures$ ,  $nClasses$ ).
13:  Set the percentage for quantum test data.
14:  Set the batch size.
15:  for all feature rows with step batch size do
16:    Split the quantum data into training and testing data.
17:    Fit the function HoeffdingTree.PARTIALFIT( $XTrain$ ,  $yTrain$ ) to the quantum training data.
18:    Predict labels for the quantum test data using the function HoeffdingTree.PREDICT( $XTest$ ).
19:    Calculate all performance metrics of the predicted labels  $yPredict$ .
20:  end for
21:  Plot performance metrics per batch.
22: end procedure

1: function QHTCDISTANCERIGETTI( $r$ )
2:   Connect to Rigetti-S using library pyquil or to Aer using library qiskit.
3:   Create a wave function simulator  $ws$ .
4:   for each data point  $p$  in feature row  $r$  do
5:     Compute qubit  $q$  as ZFeatureMap transformation of  $p$  using library pyquil (Rigetti-S) or qiskit (Aer).
6:   end for
7:   for each qubit  $q$  do
8:     Get the wave functions  $f(q)$  from  $ws$ .
9:   end for
10:  for each wave function  $f(q)$  do
11:    Compute the density matrices  $m_{f(q)}$ .
12:  end for
13:  for  $i \leftarrow 1$  to  $n$  while  $i < n$  and  $n$  is length of feature row  $r$  do
14:    Let single distances  $d_i = \text{TRACEDISTANCE}(m_{f(q)}(i), m_{f(q)}(i + 1))$ .
15:  end for
16:  Let single distance  $d_n = \text{TRACEDISTANCE}(m_{f(q)}(n), m_{f(q)}(1))$ .
17:  return Sum of single distances
18: end function

1: function TRACEDISTANCE( $m_1$ ,  $m_2$ )
2:   Let  $d = m_1 - m_2$ .
3:   Compute singular values  $s_i$  of  $d$ .
4:   return  $0.5 * \sum_i |s_i|$ 
5: end function

```

APPENDIX B. GLOSSARY

Term	Definition
API	Application Programming Interface
C&C	Command-and-Control Server
CBC	Classical Binary Classifier
COBYLA	Constrained Optimization by Linear Approximation
DGA	Domain Generation Algorithm
(D)DoS	(Distributed) Denial of Service
DL	Deep Learning
EstimatorQNN	Estimator Circuit of a Quantum Neural Network
GCP	Google Cloud Platform
HQBC	Hybrid Quantum Binary Classifier
HQDL	Hybrid Quantum Deep Learning
HTC	Hoeffding Tree Classifier
ML	Machine Learning
MLP	Multilayer Perceptron
NISQ	Noisy Intermediate-Scale Quantum
P2P	Peer-to-peer
Pegasos	Primal Estimated sub-Gradient Solver for Support Vector Machines
SPSA	Simultaneous Perturbation Stochastic Approximation
QSIEM	Quantum-enhanced Security Information and Event Management
QAOA	Quantum Approximate Optimization Algorithm
QDL	Quantum Deep Learning
QESG	Quantum Estimated Sub-Gradient
QGAN	Quantum Generative Adversarial Networks
QML	Quantum Machine Learning
QNN(C)	Quantum Neural Network (Classifier)
QCA	Quantum Cybersecurity Analytics
QSVC	Quantum Support Vector Classifier
QSVM	Quantum Support Vector Machine

Term	Definition
SamplerQNN	Sampler Circuit of a Quantum Neural Network
SIEM	Security Information and Event Management
SLSQP	Sequential Least Squares Programming optimizer
SMO	Sequential Minimal Optimization
SOAR	Security Orchestration, Automation and Response
SPSA	Simultaneous Perturbation Stochastic Approximation
SGD	Stochastic Gradient Descent
TLS	Transport Layer Security
VQC	Variational Quantum Classifier

REFERENCES

- [1] Abdulla Hussain, Azlinah Mohamed, and Suriyati Razali. A review on cybersecurity: Challenges & emerging threats. In *Proceedings of the 3rd International Conference on Networking, Information Systems & Security*, pages 1–7, 2020.
- [2] Javier Martínez Torres, Carla Iglesias Comesaña, and Paulino J García-Nieto. Machine learning techniques applied to cybersecurity. *International Journal of Machine Learning and Cybernetics*, 10:2823–2836, 2019.
- [3] Michael A Nielsen and Isaac L Chuang. Quantum computation and quantum information. *Quantum Computation and Quantum Information*, 2010.
- [4] Jacob Biamonte, Peter Wittek, Nicola Pancotti, Patrick Rebentrost, Nathan Wiebe, and Seth Lloyd. Quantum machine learning. *Nature*, 549(7671):195–202, 2017.
- [5] Ying Xing, Hui Shu, Hao Zhao, Dannong Li, and Li Guo. Survey on botnet detection techniques: Classification, methods, and evaluation. *Mathematical Problems in Engineering*, 2021.
- [6] Rakesh M. Verma and David J. Marchette. *Cybersecurity Analytics*. CRC Press, 2020.
- [7] Scott Mongeau and Andrzej Hajdasinski. *Cybersecurity Data Science: Best Practices in an Emerging Profession*. Springer, 2021.
- [8] Alessandro Parisi. *Hands-On Artificial Intelligence for Cybersecurity*. Packt Publishing, 2019.
- [9] Ravi Das. *Practical AI for Cybersecurity*. CRC Press, 2021.
- [10] Emmanuel Tsukerman. *Machine Learning for Cybersecurity Cookbook*. Packt Publishing, 2019.
- [11] Asmah Muallem, Sachin Shetty, Jan W Pan, Juan Zhao, and Biswajit Biswal. Hoeffding tree algorithms for anomaly detection in streaming datasets: A survey. *Journal of Information Security*, 8(4), 2017.
- [12] Hatma Suryotrisongko and Yasuo Musashi. Hybrid quantum deep learning and variational quantum classifier-based model for botnet dga attack detection. *International Journal of Intelligent Engineering and Systems*, 15(3):215–224, 2022.
- [13] Madjid Tehrani, Eldar Sultanow, William J Buchanan, Malik Amir, Anja Jeschke, Raymond Chow, and Mouad Lemoudden. <https://github.com/Sultanow/quantum-botnet-detection>, 2023.
- [14] Georgios Kambourakis, Marios Anagnostopoulos, Weizhi Meng, and Peng Zhou, editors. *Botnets: Architectures, Countermeasures, and Challenges*. CRC Press, 2020.
- [15] Zhichun Li, Anup Goyal, and Yan Chen. Honey-net-based botnet scan traffic analysis. In *Botnet Detection: Countering the Largest Security Threat*, pages 25–44. Springer, 2008.
- [16] Wenke Lee, Cliff Wang, and David Dagon, editors. *Botnet Detection: Countering the Largest Security Threat*. Springer, 2008.
- [17] Gernot Vormayr, Tanja Zseby, and Joachim Fabini. Botnet communication patterns. *IEEE Communications Surveys & Tutorials*, 19(4):2768–2796, 2017.
- [18] Manos Antonakakis, Tim April, Michael Bailey, Matt Bernhard, Elie Bursztein, Jaime Cochran, Zakir Durumeric, J Alex Halderman, Luca Invernizzi, Michalis Kallitsis, et al. Understanding the mirai botnet. In *26th USENIX security symposium (USENIX Security 17)*, pages 1093–1110, 2017.
- [19] Ahmed M Manasrah, Thair Khmour, and Raeda Freehat. Dga-based botnets detection using dns traffic mining. *Journal of King Saud University-Computer and Information Sciences*, 34(5):2045–2061, 2022.

- [20] Kishor Bharti, Alba Cervera-Lierta, Thi Ha Kyaw, Tobias Haug, Sumner Alperin-Lea, Abhinav Anand, Matthias Degroote, Hermanni Heimonen, Jakob S Kottmann, Tim Menke, et al. Noisy intermediate-scale quantum algorithms. *Reviews of Modern Physics*, 94(1):015004, 2022.
- [21] Félix Brezo, José Gaviria de la Puerta, Xabier Ugarte-Pedrero, Igor Santos, Pablo G. Bringas, and David Barroso. Supervised classification of packets coming from a HTTP botnet. In *2012 XXXVIII Conferencia Latinoamericana En Informatica (CLEI)*, pages 1–8. IEEE, 2012.
- [22] Giorgio Piras, Maura Pintor, Luca Demetrio, and Battista Biggio. Explaining machine learning DGA detectors from DNS traffic data. <https://arxiv.org/abs/2208.05285>, 08 2022.
- [23] Zhi-Juan Jia, Ning Wang, Yun-Ye Wang, and Ming-Sheng Hu. The traceability analysis and research of botnet control center based on ant colony group-dividing algorithm. In *2018 13th IEEE Conference on Industrial Electronics and Applications (ICIEA)*. IEEE, 2018.
- [24] Manuel Gil Pérez, Alberto Huertas Celdrán, Fabrizio Ippoliti, Pietro G. Giardina, Giacomo Bernini, Ricardo Marco Alaez, Enrique Chirivella-Perez, Félix J. García Clemente, Gregorio Martínez Pérez, Elian Kraja, Gino Carrozzo, Jose M. Alcaraz Calero, and Qi Wang. Dynamic reconfiguration in 5G mobile networks to proactively detect and mitigate botnets. *IEEE Internet Computing*, 21(5):28–36, 2017.
- [25] Patrick Onotu, David Day, and Marcos Rodrigues. Accurate shellcode recognition from network traffic data using artificial neural nets. In *The 28th Canadian Conference on Electrical and Computing Engineering (CCECE)*, pages 355–360, 2015.
- [26] Pascal Maniriho, Abdun Naser Mahmood, and Mohammad Javed Morshed Chowdhury. Evaluation and survey of state of the art malware detection and classification techniques: Analysis and recommendation. <http://dx.doi.org/10.2139/ssrn.4197678>, 2022.
- [27] Gennaro De Luca. A survey of nisq era hybrid quantum-classical machine learning research. *Journal of Artificial Intelligence and Technology*, 2(1):9–15, 2022.
- [28] Michael Broughton, Guillaume Verdon, Trevor McCourt, Antonio J Martinez, Jae Hyeon Yoo, Sergei V Isakov, Philip Massey, Ramin Halavati, Murphy Yuezhen Niu, Alexander Zlokapa, et al. Tensorflow quantum: A software framework for quantum machine learning. *arXiv preprint arXiv:2003.02989*, 2020.
- [29] Hatma Suryotrisongko, Yasuo Musashi, Akio Tsuneda, and Kenichi Sugitani. Adversarial robustness in hybrid quantum-classical deep learning for botnet DGA detection. *Journal of Information Processing*, 30:636–644, 2022.
- [30] Maxim Kalinin and Vasilij Krundyshev. Security intrusion detection using quantum machine learning techniques. *Journal of Computer Virology and Hacking Techniques*, 2022.
- [31] Hatma Suryotrisongko. Botnet DGA Dataset. <https://dx.doi.org/10.21227/rg6z-z622>, 05 2020.
- [32] H Suryotrisongko. Botnet dga detection. *IEEE Code Ocean*, 2021.
- [33] Mattia Zago, Manuel Gil Pérez, and Gregorio Martínez Pérez. Umudga: A dataset for profiling algorithmically generated domain names in botnet detection. *Data in Brief*, 30:105400, 2020.
- [34] R. Livni I. Amir, T. Koren. Sgd generalizes better than gd (and regularization doesn't help). *arXiv2 preprint arXiv:2102.01117*, 2022.
- [35] Pedro Domingos and Geoff Hulten. Mining high-speed data streams. In *Proceedings of the sixth ACM SIGKDD international conference on Knowledge discovery and data mining*, pages 71–80, 2000.
- [36] Wassily Hoeffding. Probability inequalities for sums of bounded random variables. *Journal of the American Statistical Association*, 58:13–30, 1963.

- [37] Oded Maron and Andrew W. Moore. Hoeffding races: Accelerating model selection search for classification and function approximation. In J. D. Cowan, G. Tesauro, and J. Alspecter, editors, *Advances in Neural Information Processing Systems*, volume 6, pages 59–66. Morgan Kaufmann Publishers, San Francisco, CA, 1994.
- [38] Jacob Montiel, Jesse Read, Albert Bifet, and Talel Abdessalem. Scikit-multiflow: A multi-output streaming framework. *Journal of Machine Learning Research*, 19(72):1–5, 2018.

LIST OF FIGURES

- 1 Stabilized architecture of experiments on real quantum devices comprising of three components Google Cloud, Azure and Azure Quantum Providers. 11
- 2 Stabilized architecture for QHTC experiments on quantum simulators Aer and Rigetti-S. The difference in implementation originates from differences in library functionalities available on Aer and Rigetti-S. 11
- 3 Quantum-enhanced SIEM. The individual steps are marked with numbers in red circles and are explained in List 2 13
- 4 PegasusQSVC's accuracy on quantum simulator AER with (a) a batch size of 100 data samples does not improve its accuracy with an increased number of batches, unlike (b) a batch size of 1,000 data samples. 14

LIST OF TABLES

- 1 Naming conventions for selected platforms shown with their machine name and their device mode (quantum simulator, real-device-based simulator, or real quantum device) 8
- 2 Selected descriptive statistics of the IEEE Botnet DGA Dataset [31] for the seven features according to the Anderson-Darling normality test. 9
- 3 Performance results in terms of accuracy and total execution time T_{total} of real quantum devices, using 100 data samples for all runs. For each algorithm and platform, the choice of the feature map and the optimizer is also shown. 16
- 4 Performance results in terms of accuracy and total execution time T_{total} of quantum simulator and real-device-based simulator experiments, using 5,000 data samples for QHTC, and 1,000 data samples for all other algorithms. For each algorithm and platform, the choice of the feature map and the optimizer is also shown. 17
- 5 Metric results in terms of accuracy, F1-score and AUC for algorithm QHTC, displayed for 5 batches with 1,000 data samples each and their average. 18

LIST OF REFERENCED LISTS

1	Reasons for instability	10
2	Steps in the solution architecture	12

MADJID G. TEHRANI, GEORGE WASHINGTON UNIVERSITY, WASHINGTON, DC 20052, USA
Email address: madjid_tehrani@gwu.edu

ELDAR SULTANOW, CAPGEMINI DEUTSCHLAND GMBH, NUREMBERG, GERMANY
Email address: eldar.sultanow@capgemini.com

WILLIAM J BUCHANAN, EDINBURGH NAPIER UNIVERSITY, EDINBURGH, UK
Email address: b.buchanan@napier.ac.uk

MALIK AMIR, MCGILL UNIVERSITY, UNIVERSITÉ DE MONTRÉAL, MONTREAL, CANADA
Email address: malik.amir.math@gmail.com

ANJA JESCHKE, CAPGEMINI DEUTSCHLAND GMBH, HAMBURG, GERMANY
Email address: anja.jeschke@capgemini.com

RAYMOND CHOW, GEORGE WASHINGTON UNIVERSITY, WASHINGTON, DC 20052, USA
Email address: laserray@gwu.edu

MOUAD LEMOUDDEN, BLOCKPASS ID LAB, EDINBURGH NAPIER UNIVERSITY, EDINBURGH, UK
Email address: m.lemoudden@napier.ac.uk